


Nonlinear absorption of ultrashort ultrahigh intensity laser pulses in fullerene

Cite as: AIP Advances **8**, 125016 (2018); <https://doi.org/10.1063/1.5042300>

Submitted: 31 May 2018 • Accepted: 08 September 2018 • Published Online: 19 December 2018

 U. Chakravarty and Deepa Chaturvedi



View Online



Export Citation



CrossMark

ARTICLES YOU MAY BE INTERESTED IN

[Femtosecond laser three-dimensional micro- and nanofabrication](#)

Applied Physics Reviews **1**, 041303 (2014); <https://doi.org/10.1063/1.4904320>

[Radially polarized optical vortex converter created by femtosecond laser nanostructuring of glass](#)

Applied Physics Letters **98**, 201101 (2011); <https://doi.org/10.1063/1.3590716>

[Mechanism of heat-modification inside a glass after irradiation with high-repetition rate femtosecond laser pulses](#)

Journal of Applied Physics **108**, 073533 (2010); <https://doi.org/10.1063/1.3483238>

Read Now!

AIP Advances

Materials Science Collection

Nonlinear absorption of ultrashort ultrahigh intensity laser pulses in fullerene

U. Chakravarty^{1,2,a} and Deepa Chaturvedi³

¹Laser Plasma Section, Raja Ramanna Centre for Advanced Technology, Indore 452013, India

²Homi Bhabha National Institute, Training School Complex, Anushaktinagar, Mumbai 400094, India

³Indian Institute of Technology, Delhi 110016, India

(Received 31 May 2018; accepted 8 September 2018; published online 19 December 2018)

Non linear absorption of intense few cycle laser pulses in fullerenes is studied by treating it as a laser driven nonlinear oscillator, using a rigid shell model. Efficient collisionless absorption of intense (Intensity $I < 10^{18}$ W/cm²) ultrashort laser pulses in fullerene (C₆₀) is estimated owing to its extraordinary anharmonicity which is quite different than the conventionally used solid gas clusters. Compared to gas clusters nonlinear resonance in C₆₀ has unusual characteristics. Factors other than nonlinear resonance which contribute in energy absorption in C₆₀ are outlined. Strong dephasing of electrons with the laser field both at onset and during the dynamical oscillations leads to the efficient energy gain by the electrons. It is found that fullerene has a distinct threshold intensity requirement depending on its charge for efficient absorption. These properties make fullerene unique for efficient absorption of high intensity few cycle laser pulses. © 2018 Author(s). All article content, except where otherwise noted, is licensed under a Creative Commons Attribution (CC BY) license (<http://creativecommons.org/licenses/by/4.0/>). <https://doi.org/10.1063/1.5042300>

INTRODUCTION

Coupling of high intensity ultrashort laser pulse energy in matter for efficient x-ray,¹ electron and high energy ion generation is of great interest for various applications.² Solid spherical clusters (SC) and Nanostructures are a promising solution to the challenge of inefficient absorption of intense lasers.³⁻⁵ Since plasma becomes collisionless at high temperature and intensity collisionless absorption mechanisms need to be used effectively. Generally absorption dynamics in laser cluster/nanoparticle interaction is understood by the oscillator model, where the cluster charge density oscillation is driven by the incident laser field.⁴⁻⁷ Absorption drastically enhances on excitation of linear resonances where the incident laser frequency ω matches the natural frequency of spherical electron cloud oscillation $\omega_p/\sqrt{3}$ (ω_p is the plasma frequency $= (ne^2/m\epsilon_0)^{1/2}$).^{6,7} Fulfillment of this condition requires sufficient cluster expansion for electron density (n) dilution to meet the resonance condition. For efficient radiation and particle generation it is desirable to couple the high intensity laser pulse energy at solid density. It has been shown that efficient coupling of energy in solid density matter can be achieved by exciting the non linear resonance (NLR).⁷⁻¹⁰ As is well known that in nonlinear oscillator problems, the oscillation frequency depends on amplitude. At high intensity the amplitude of electron cloud oscillation becomes very high, which lowers the restoring force of electron cloud. This leads to the decrease of the instantaneous electron cloud oscillation frequency ($\Omega(t)$). Therefore the non linear resonance condition $\Omega(t)=\omega$ ($\omega=2\pi c/\lambda$) is dynamically met during the oscillations. This model has also been successfully validated in PIC (particle in cell simulations)⁸ and has also explained many experimental results.¹¹ In the quest for exotic targets showing varied response to ultrashort pulses fullerene is also used as target.^{5,12} Fullerene (C₆₀) has a single layer spherical/caged molecular structure that is easily produced in intense laser irradiated graphite. Fullerene has been shown to

^auday@rccat.gov.in

be an excellent target for water window X-ray and High harmonic generation.^{5,12-14} The hollow structure of fullerene is expected to have a very different response than the solid clusters when subjected to intense pulses. In this paper we analytically model the coherent collective oscillations of electrons of fullerene in response to intense few cycle pulses. It is found that the electron cloud oscillation dynamics of fullerene is quite distinct from the usual non linear oscillations in laser interacting with SC.⁷⁻¹⁰ The motion is highly anharmonic at all amplitudes as compared to SC. The absorption critically depends on the laser intensity, number of laser cycles, degree of ionization and the fullerene geometry. The analysis shows that fullerenes have a characteristic threshold of the incident laser electric field strength for finite absorption. It is also found there is an optimum intensity for maximum absorption that depends on the degree of ionization. NLR characteristics of C₆₀ and dephasing of electron with laser field is very different compared to SC.^{7,10,15} This makes fullerene a very attractive target for ionization studies,¹⁶⁻¹⁸ absorption,⁵ high harmonic generation^{12,13} and is also a naturally suitable candidate for few cycle interactions.¹³ The broadband HHG from fullerenes^{13,14} can also be easily understood qualitatively by this model. In general the model is also applicable to many fullerene like structures (C₂₀, C₃₀, C₁₈₀ etc) and can be extended to study the dynamics of laser interaction with single layer structures like single walled Carbon Nanotubes and Graphene.

THE RIGID SHELL MODEL FOR FULLERENE

The analytical model for predicting the complex ionization dynamics of fullerene in low intensity laser field ($\approx 10^{13-14}$ W/cm²) was discussed by Bhardwaj et.al.,¹⁸ they considered electron moving in a potential of a conductor sphere. The present study however is intended to bring out the collective absorption dynamics of more intense laser in C₆₀. Our model is based on self consistent laser interaction with two overlapping thin conductor shells over much large range of intensities ($I=10^{12-18}$ W/cm²). At high intensities $I \gg 10^{14}$ W/cm² the ionization Q in C₆₀ is high as electrons are freed from the individual Carbon sites at the foot of the intense laser pulse. Subsequent to the ionization the electron shell which is bound to the caged fullerene ion shell core may start moving under the effect of the incident field of sufficient strength. A simplistic classical description based on the correspondence principle is enlightening to bring out the dynamics of the absorption processes involved.^{7,9,10} Assuming a rigid shell model the electrons shell freed from the bucky ball surface structure move coherently and collectively under the effect of the incident laser field. Using simple yet detailed calculations based on the Gauss's law and elementary laws of electrostatics we first evaluate the integrated force between the ion and electron shell as function of Δ . Where Δ is the amplitude of oscillation or the distance between the ion and the electron shell centre. Very interestingly it is found that, when the oscillation amplitude is less than $2R$ the force of attraction is constant meaning it is independent of the amplitude. The Fig. 1(a) shows the cross-section of two intersecting shells of ion and electron both of radius R and carrying charge $+Q$ and $-Q$. The distance between their centers A (for ion shell) and B (for electron shell) is Δ . The aim is to find the force of attraction between the mobile electron shell due to the stationary ion shell. A spherical Gaussian surface is drawn just outside the ion shell shown in dotted form (This Gaussian shell should be just outside the ion shell though for visual clarity in the schematic it is shown a little larger than the ion shell). The curved portion EF of electron shell lying inside the ion shell does not feel any force due to the ion shell since the electric field inside the ion shell $E_{in}=0$ (This is well known that electric field inside a charged shell is zero from Gauss law). The portion of electron shell outside the ion shell and also the spherical Gaussian surface (the curved region ECDF) experiences force due to the ion shell. Again using the Gauss law the charge $+Q$ of the spherical ion shell can be assumed to be located at point A which is the centre of ion shell provided one is seeing its effect outside the Gaussian surface. With these arguments the problem is simplified to finding the force experienced by electron shell outside the Gaussian surface (ECDF) due to $+Q$ charge located at point A which is the ion shell centre. This is shown more clearly in the Fig. 1(b). The net force of attraction between $+Q$ and electron shell portion outside the Gaussian surface can be found by dividing electron shell further into elementary rings at different locations z from A. The charge $+Q$ is located at A which is at the axis of the ring as shown in Fig. 1(c). Any arbitrary point C located on this elementary ring is such that AC and BC makes

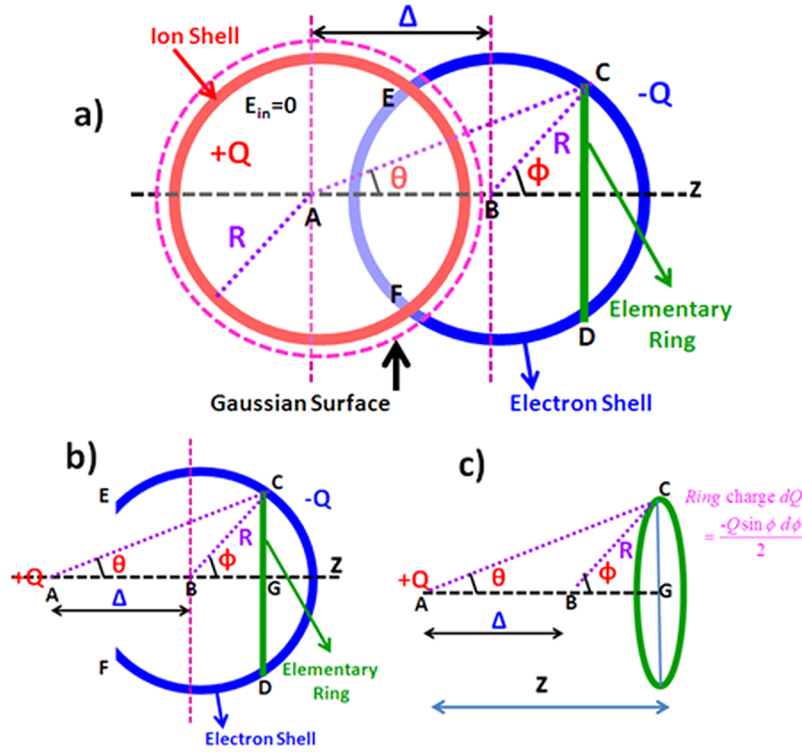


FIG. 1. (a) The side cross-section of intersecting ion and electron shells of radius R carrying charge $+Q$ and $-Q$ respectively. The distance between the shell centers A and B is Δ . A Gaussian sphere is drawn just outside the ion sphere shown in dotted for. (b) The problem of finding the force of attraction between the two opposite charged overlapping shells is reduced to an equivalent charge $+Q$ placed at the centre of ion sphere and portion of electron sphere outside the Gaussian surface. (c) The electron shell can be further divided in to circular elementary rings of radius $r=R \sin \phi$ located at distance $z= \Delta+R \cos \phi$.

an angle θ and ϕ with respect to the z axis. The radius of the ring is “ r ” and its location is at “ z ” with respect to point A . Radius of the elementary ring $r=R \sin \phi$ and its location $z=\Delta+R \cos \phi$. Let us first find the charge on the elementary ring. The surface charge density of charged electron sphere is $-Q/4\pi R^2$, area of the elementary ring is $\{2\pi(R \sin \phi)R d\phi\}$. Therefore charge dQ on elementary ring is $-\{(Q/4\pi R^2)2\pi(R \sin \phi)R d\phi\}$ is given in equation (1).

$$\text{ring charge } dQ = \frac{-Q \sin \phi d\phi}{2} \quad (1)$$

The horizontal force dF along z axis on this elementary ring due to $+Q$ charge at A is given in equation (2) (Note the component of forces perpendicular to z axis cancel and only the horizontal forces add). Here we use the fact that, the charge contained in $dl=dQ/2\pi r$ and $\cos \theta=z/(r^2+z^2)^{1/2}$.

$$dF = \int \frac{1}{4\pi\epsilon_0} \frac{Qz}{(r^2+z^2)^{3/2}} \frac{dQ}{2\pi r} dl \quad (2)$$

Here dl is the length element chosen from the elementary ring ($\oint dl = 2\pi r$), this leads to eq. (3)

$$dF = \frac{1}{4\pi\epsilon_0} \frac{Qz}{(r^2+z^2)^{3/2}} \frac{dQ}{2\pi r} 2\pi r \quad (3)$$

Putting the values of r and z in eq. (3) and using eq. (1) for value of dQ give eq. (4)

$$dF = \frac{1}{4\pi\epsilon_0} \frac{Q(\Delta + R \cos \phi)}{(R^2 \sin^2 \phi + (\Delta + R \cos \phi)^2)^{3/2}} \frac{-Q \sin \phi d\phi}{2} \quad (4)$$

Finally the net force of attraction between +Q and the electron shell portion outside the Gaussian surface is given by integrating dF under proper limits. For finding the limits of ϕ it may be noted that line joining EF is located at $-\Delta/2$ from B)

$$F = \int_0^{\cos^{-1}(-\Delta/2R)} -\frac{1}{8\pi\epsilon_0} Q^2 \frac{(\Delta + R \cos \phi)}{(R^2 + \Delta^2 + 2\Delta R \cos \phi)^{3/2}} \sin \phi d\phi \quad (5)$$

ϕ changes from 0 to $\cos^{-1} - \frac{\Delta}{2R}$
Choosing $R \cos \phi = t$

$$F = \frac{Q^2}{8\pi\epsilon_0 R} \int_R^{-\Delta/2} \frac{(\Delta + t)}{(R^2 + \Delta^2 + 2\Delta t)^{3/2}} dt \quad (6)$$

changing the variable to $y = R^2 + \Delta^2 + 2\Delta t$

$$F = \frac{Q^2}{8\pi\epsilon_0 R} \int_{(R+\Delta)^2}^{R^2} \left(\Delta + \frac{(y - R^2 - \Delta^2)}{(2\Delta)} \right) y^{-3/2} \frac{dy}{2\Delta} \quad (7)$$

$$F = \frac{Q^2}{32\pi\epsilon_0 R \Delta^2} \int_{(R+\Delta)^2}^{R^2} (y^{-1/2} + (\Delta^2 - R^2)y^{-3/2}) dy \quad (8)$$

$$F = \frac{Q^2}{32\pi\epsilon_0 R \Delta^2} [2y^{1/2} - 2(\Delta^2 - R^2)y^{-1/2}]_{(R+\Delta)^2}^{R^2} \quad (9)$$

Putting the Limits simplifies the equation and yields an amplitude independent force given in equation (10)

$$\begin{aligned} F &= \frac{Q^2}{32\pi\epsilon_0 R \Delta^2} \left[\left(2R - \frac{2(\Delta^2 - R^2)}{R} \right) - \left(2(R + \Delta) - \frac{2(\Delta^2 - R^2)}{(R + \Delta)} \right) \right] \\ F &= \frac{Q^2}{32\pi\epsilon_0 R \Delta^2} \left(\frac{-2\Delta^2}{R} \right) \\ F &= -\frac{Q^2}{16\pi\epsilon_0 R^2} \end{aligned} \quad (10)$$

This surprising finding of amplitude independent constant force which is counter intuitive to some extent can also be understood physically. As the electron shell moves out (increase of Δ), more and more electron charge comes outside the Gaussian surface and starts seeing the attractive force of the ion shell. But the distance Δ between the ion core centre and the electron shell cloud also increases due to the electron shell motion. These two effects that is increase of effective charge (more Coulomb force) seeing the attraction and increasing distance (less Coulomb force) exactly compensate and cancel in case of fullerene like structures. After finding the integrated force of attraction between electron and ion shell of fullerene the equation of motion of electron shell under applied field $E(t)$ is given in eq. (11) (mass of electron shell is M).

$$M\ddot{\Delta} + \text{sgn}(\Delta) \left(\begin{array}{l} \frac{Q^2}{16\pi\epsilon_0 R^2} ; \text{ for } -2 < \frac{\Delta}{R} < 2 \\ \frac{Q^2}{4\pi\epsilon_0 \Delta^2} ; \text{ for } \left| \frac{\Delta}{R} \right| \geq 2 \end{array} \right) = -QE(t) \quad (11)$$

A constant force $Q^2/(16\pi\epsilon_0 R^2)$ directed towards the ion core is what makes this oscillator a fascinating one. Once the amplitude of oscillation exceeds $2R$ the force experienced by the electrons is simply $Q^2/(4\pi\epsilon_0 \Delta^2)$. Fig. 2(a) shows the overlapping electron and ion shell of radius R (diameter $2R=0.7 \text{ nm}$ for fullerene) carrying charge $+Q$ and $-Q$ respectively. The force experienced by

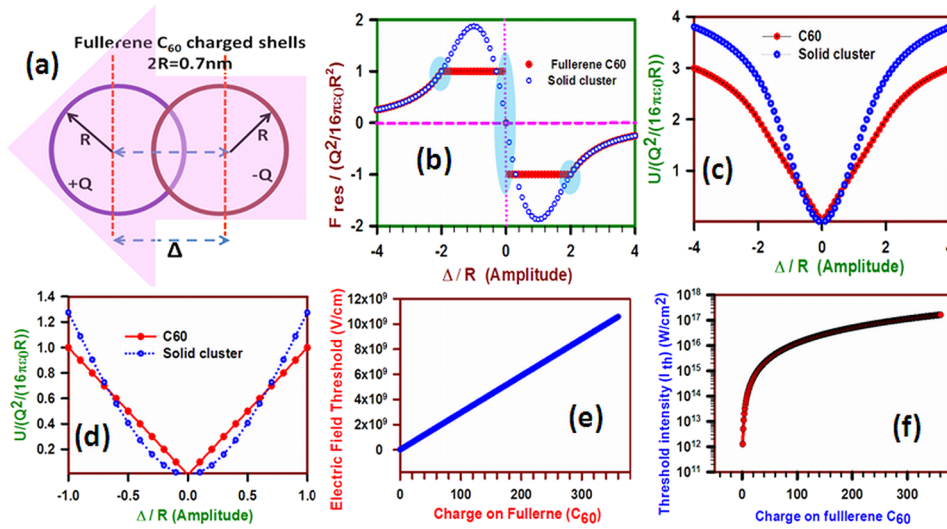


FIG. 2. (a) The diagram of overlapping ion (+Q) and electron shell (-Q), the electron shell is oscillating about the ion shell under the effect of intense laser field. (b) The restoring force vs amplitude for fullerene and solid gas cluster for comparison. The shaded regions are the points where electron shell of C_{60} gets strong dephasing resulting from abrupt force profile change at origin and boundary. This effect is negligible for solid gas clusters owing to smooth force profile. (c) Potential energy of electron vs amplitude of oscillation of fullerene and solid gas clusters for comparison. (d) Fig (c) is zoomed to show the stiffness of fullerene oscillator at low amplitude. (e) The threshold electric field strength for onset of nonlinear oscillations vs Charge on fullerene. (f) The threshold intensity vs charge on fullerene for finite absorption.

the electrons is shown in Fig. 2(b) and for comparison the case of SC is also shown from known relation written in the following form $F(\Delta)/(Q^2/16\pi\epsilon_0 R^2) = -4\text{sgn}((\Delta/R) - (9/16)(\Delta/R)^2 + (1/32)(\Delta/R)^4)$ for $|\Delta| \leq 2R$ $-4\text{sgn}(R^2/\Delta^2)$ for $|\Delta| \geq 2R$.⁸⁻¹⁰ Clearly the force profile of SC is very smooth in comparison to C_{60} . In fullerene there are abrupt force changes at origin and at $\Delta \pm 2R$ (boundary) as shown in the shaded region seen from Fig. 2(b). Naturally due to the abrupt acceleration at these points a huge dephasing (non-adiabaticities) occur. Now, the electric field must exceed the threshold (E_{th}) of $Q/(16\pi\epsilon_0 R^2)$ for the electron motion to begin. This implies a natural dephasing between the incident laser field E and the consequent current of the resultant motion. Poynting's theorem states that, for absorption of light in matter there must be a finite dephasing between light field (E) and the resultant current density (J).^{10,15} A constant force is the manifestation of linear potential energy (U) shown in eq. (12). The equation shows the potential energy of C_{60} has different amplitude dependence for $-2R < \Delta < 2R$ and $\Delta > 2R$ and $\Delta < -2R$.

$$\frac{U(\Delta)}{Q^2/4\pi\epsilon_0 R} = \begin{cases} \frac{|\Delta|}{R} & |\Delta| \leq 2R \\ 4 - \frac{4R}{|\Delta|} & |\Delta| > 2R \end{cases} \quad (12)$$

Fig. 2(c) shows the potential energy of fullerene electrons by plotting equation (12) along with the potential energy of solid clusters derived using the results of Kundu et. al.⁸

$U(\Delta)/(Q^2/4\pi\epsilon_0 R) = 2(\Delta/R)^2 - (3/4)(\Delta/R)^3 - (1/40)(\Delta/R)^5$ for $|\Delta| \leq 2R$ and $24/5 - 4R/\Delta$ for $|\Delta| > 2R$. Nearly harmonic motion is expected due to a near quadratic potential for low amplitude of oscillations in SC as evident from a zoomed version of Fig. 2(c) shown in Fig. 2(d). At high amplitude the potential lowers for both particles (SC and C_{60}) making it a soft oscillator and the instantaneous oscillation frequency lowers. It is seen that fullerene anharmonicity is very peculiar, it is a stiff nonlinear oscillator at low amplitudes. Whereas, at high amplitude the fullerene oscillator becomes softer than SC as seen from Fig. 2(c) and 2(d). The C_{60} molecule has a distinct electric field threshold $Q/(16\pi\epsilon_0 R^2)$ and therefore a finite absorption is always there even without a collision term provided the incident field strength surpasses the threshold value. High charge/ionization has higher electric field threshold as also seen from Fig. 2(e).

The typical intensity threshold (I_{th}) for the onset of motion can be readily found by equalizing the laser field strength E with E_{th} ($E = E_{th}$) and is obtained from eq. (13)

$$I_{th} = \frac{cQ^2}{512\pi^2\epsilon_0R^4} \quad (13)$$

Plugging the constants for C_{60} $I_{th}=1.26 \times 10^{12} \text{W/cm}^2 \times (\text{Total charge on fullerene/charge of electron})^2$, I_{th} is also shown in Fig. 2(f). It may be pointed here I_{th} is quite close to the tunnel ionization threshold (for $Q \gg 1e$) of C_{60} predicted analytically^{16,17} and measured experimentally by other groups for $10^{13} \text{W/cm}^2 < I < 10^{14} \text{W/cm}^2$.^{16,18}

On the threshold crossing and onset of oscillation in C_{60} as the amplitude grows it becomes a soft oscillator and the instantaneous frequency is lowered. It readily equals the incident laser frequency ω , and the NLR condition is met.^{7,8} Interestingly, unlike SC the natural amplitude dependent Time period $T/\text{frequency}$ ($\Omega_0 = 2\pi/T_0$) of undriven fullerene oscillator can be easily calculated analytically. To look for the possibility whether a non linear oscillator can meet the resonance condition, analytical expression for amplitude dependent time period is very useful. It helps in anticipating the laser intensity requirement to meet NLR for a chosen incident wavelength and given target ionization and geometry. The amplitude dependent natural frequency (frequency of undriven oscillator) is found by choosing $\Delta(t=0) = A$; $\dot{\Delta}(t=0) = 0$. That is the initial amplitude A and the initial velocity of the electron shell is zero. As larger and larger amplitude is chosen T_0 keeps on increasing. This implies that the natural frequency decreases monotonically and at some value of initial amplitude this frequency can become equal to the laser frequency ω . T_0 is found using equation (14) as a function of initial amplitude, and other parameters.

$$T_0 = \left(\begin{array}{l} 4\sqrt{\frac{A}{\alpha}} \quad |A| \leq 2R \\ 4\left(\frac{A^{3/2}}{\sqrt{2\beta}} \sin^{-1} \sqrt{1 - \left(\frac{2R}{A}\right)} + \sqrt{\frac{2R}{A} \left(1 - \frac{2R}{A}\right)}\right) + \frac{-v_{2R} + \sqrt{v_{2R}^2 + 4\alpha R}}{\alpha} \quad |A| > 2R \end{array} \right) \quad (14)$$

Where $\alpha = \frac{Q^2}{16\pi\epsilon_0R^2M}$, $\beta = \frac{Q^2}{4\pi\epsilon_0M}$ and $v_{2R} = \sqrt{2d(A-2R)/2AR}$.

As seen from equation (14) Possibility of excitation of NLR in fullerene is expected since larger "A" implies lowering of the natural frequency ($\Omega_0=2\pi/T_0$) and it may become equal to incident laser frequency ω . Higher charge and larger wavelength require high amplitude and therefore higher intensity is a prerequisite for NLR in such cases.

However, to get a true picture of oscillation dynamics and whether NLR can occur in fullerenes it must be driven by an incident laser field $E(t)$. Equation (11) can be written in the form given by $\ddot{\Delta} + \Omega_{eff}^2\Delta = -QE(t)/M$ where the instantaneous effective oscillation frequency $\Omega_{eff}(t)$ is given by Eq. (15) for different regions. NLR occurs when $\Omega_{eff}(t)=\omega$.⁸

$$\Omega_{eff}(t) = \left(\begin{array}{ll} \left(\frac{Q^2}{4\pi\epsilon_0R^2M|\Delta|}\right)^{1/2} & 0 < |\Delta| \leq 2R \\ 0 & \Delta = 0 \\ \left(\frac{Q^2}{4\pi\epsilon_0M|\Delta|^3}\right)^{1/2} & |\Delta| > 2R \end{array} \right) \quad (15)$$

It is clear from the equation (15) as well that $\Omega_{eff}(t)$ decreases with instantaneous amplitude for different charge on fullerene. It also clearly points out that high charge NLR is met after the shells separate ($\Delta > 2R$). Naturally this implies that as the amplitude of oscillation grows, at the boundary additional strong dephasing kick may be encountered (as seen from Fig. 2(b)) before achieving NLR. For low values of Q , NLR may be met for $\Delta < 2R$ and NLR occurs before strong acceleration changes occur at boundary. In SC electron cloud becomes free exactly at NLR,⁸ however C_{60} does not exhibit this property. Though in the vicinity of NLR absorption starts increasing and eventually the electron shell sets free while meeting the NLR condition in the process of energy gain.

RESULTS ON NONLINEAR ABSORPTION OF INTENSE ULTRA-SHORT PULSES IN FULLERENE

We studied the dynamical laser energy absorption process in fullerene when it is irradiated by a laser field $E(t) = -E_0 \sin^2(\omega t/2N) \cos(\omega t)$ (N is the number of cycles).⁸ It is important to mention for $N \leq 1$ (subcycle pulses), a more accurate description of pulse is required otherwise an excess energy gain of a factor greater than 2 is obtained.¹⁹ Pulses of varying strength and number of cycles were used to drive this non linear oscillator for different degree of ionization (1-6 for carbon atoms corresponding to a total charge of 60,120,180,240,300 and 360). Just for comparison, we also take the total charge of fullerene as 1, 5, 20 for the case when ionization is low (for low intensity laser pulse). The term $Q \cdot v(t) \cdot E(t)$ is the absorption rate and its time integral gives the net absorbed energy. The instantaneous velocity $v(t)$ is the time derivative of $\Delta(t)$. The Absorbed energy is calculated by solving the equation of motion using equation (11). Instantaneous velocity $v(t)$ is numerically evaluated, subject to the initial condition $\Delta(t=0) = 0$; $\dot{\Delta}(t=0) = 0$. The laser energy absorbed by a single electron in an N cycle laser during the pulse (pulse duration $T = 2\pi N/\omega$) is calculated by the integral $\int_0^T v(t) \cdot E(t) dt$. A high absorption was estimated in fullerenes, and it depends on the Q , E , N , and λ . Fig. 3(a)–3(d) shows the energy absorbed per electron per unit laser pondermotive energy $U_p = 9.33 \times 10^{-14} (W/cm^2) \lambda(\mu m)^2$ (in eV). We take the case of Ti: Sapphire laser having $\lambda = 800$ nm. The energy absorbed per electron per unit laser pondermotive energy for different charge on fullerene (+1,+5,+10,+20,+60,+120,+180,+240,+300,+360) vs the incident laser intensity for different number of laser cycles (a) $N = 1$ cycle (b) $N = 2$ cycle (c) $N = 5$ cycle (d) $N = 10$ cycle is depicted in Fig. 3(a)–3(d). The Fig. 3(a)–3(d) also depicts that the absorption is efficient and maximizes at a particular intensity I_{max} above the threshold I_{th} depending on the degree of ionization. The reason for the efficient absorption in fullerenes is primarily due to the threshold nature of interaction. The natural dephasing between the driver laser and the electron response results in a finite absorption. For high Q absorption optimizes at high Intensity (I_{max} is higher) and for low Q absorption maximizes at low

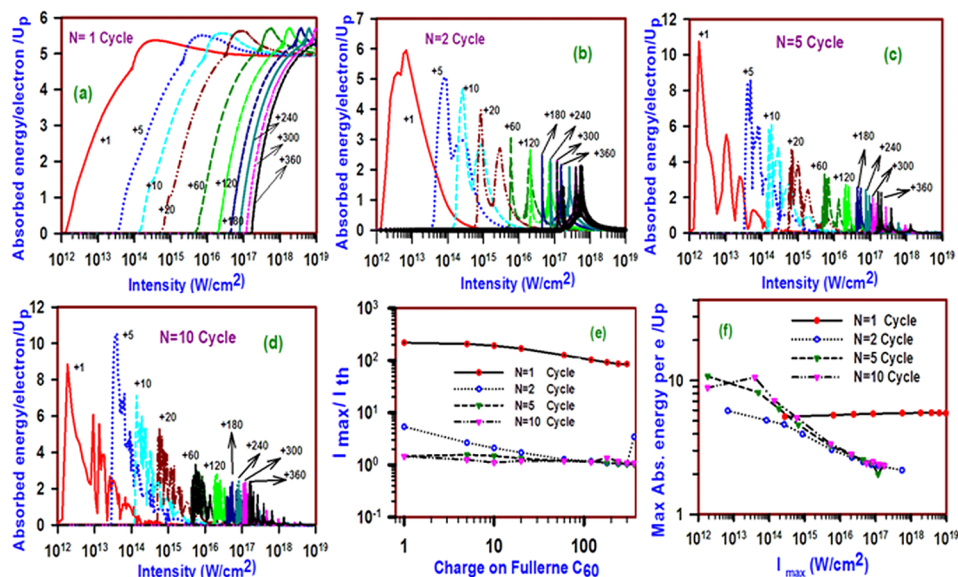


FIG. 3. Energy absorbed per electron per U_p (pondermotive energy) for different charge (+1,+5,+10,+20,+60,+120,+180,+240,+300,+360) vs the incident laser intensity (800 nm light). Various sine square laser pulses of different number of cycles (N) drive the nonlinear oscillation of fullerene electrons. (a) $N = 1$ cycle (b) $N = 2$ cycle (c) $N = 5$ cycle (d) $N = 10$ cycle. Results summarizing the graphs (a) to (d) shown in (e) and (f). (e) The intensity at which absorbed energy becomes maximum, is normalized to the threshold intensity and the graph is plotted for various Q and for different number of cycles. As seen from Fig. (e) for $N > 1$ and $Q > 5$ absorption maximizes just above I_{th} . (f) Maximum absorbed energy per electron per U_p for various number of cycles (The points from left to right correspond to different charge (+1,+5,+10,+20,+60,+120,+180,+240,+300,+360)). Maximum absorption is almost independent of number of cycles and is similar for same Q (for $Q > 5$); for $N > 1$ maximum absorption gradually decrease for high Q .

intensity in general. On increasing the number of cycles absorption at high intensity reduce gradually as seen from the Fig. 3(b)–3(d). For moderate intensities, low Q and few cycle pulses the absorption is remarkably high. This rigid oscillator exhibits high absorption just above I_{th} (the threshold intensity for onset of motion) for larger N and Q (see Fig. 3(c) and 3(d)). Whereas for smaller N absorption maximizes much above I_{th} (see Fig. 3(a) and 3(b)). This is summarized in Fig. 3(e) which shows I_{max}/I_{th} variation vs charge. The value is just above and close to 1 for high Q and high N . Efficient absorption still exists when $I \gg I_{max}$ to some extent. The collisionless absorption/irreversible energy gain by the electrons may also proceed through anharmonic resonances in C_{60} similar to SC.^{7,8,10} As mentioned earlier after the onset of motion, as the amplitude of electron shell increases this oscillator becomes softer. This is evident from restoring force and potential profile seen in Fig. 2(b)–2(d). NLR in C_{60} condition can be easily met at comparatively lower intensity than SC owing to the weak restoring force (for $\Delta > R/4$ restoring force in fullerene becomes less than that of SC). This explains the sharp rise of absorption beyond I_{th} in C_{60} . The Non linear dynamic analysis of the motion revealed that fullerene response is very different from solid clusters. In laser irradiated solid clusters at NLR the electron sphere leaves the solid ion sphere. However, in the case of fullerene NLR is not the only dominant factor. Electron shell cloud becomes free in fullerene depending on phase of pulse in the vicinity of NLR, its intensity, and charge Q . Interestingly, the laser frequency and instantaneous oscillation frequency become equal multiple times in some cases (This happens only once in SC). Nevertheless, the condition for maximum energy transfer from laser to electrons happens in temporal proximity of NLR confirming that laser phase and intensity are very crucial for energy coupling in this highly dynamical oscillator. The reason for this difference from SC may be simply understood from Fig. 2(b), which shows that a huge change in restoring force at origin, and at $\Delta = \pm 2R$ causes drastic change in acceleration and hence dephasing (sometimes multiple times). Even though dephasing is important criterion for absorption which can easily be satisfied in C_{60} oscillator. But for maximum energy gain the electron must be in at proper energy gaining phase for a prolonged time. Evidently large Q and N cases show a chaotic pattern in absorption at high intensities (Fig. 3(c) and 3(d)). This happens due to multiple dephasing in every cycle at cluster boundary and at origin. Since for high Q , NLR can be met only if $\Delta > 2R$ and therefore dephasing at boundary cannot be avoided. Fig. 3(f) shows the summary of the observations of Fig. 3(a)–3(d). Where the maximum absorbed energy per electron per U_p at different intensities I , N and Q are shown. As the number of cycle increases the maximum absorbed energy decrease monotonically for any chosen value of Q . The maximum absorbed energy is almost independent of N and it is noted that for large Q absorption is quite high ($2-3U_p$) in the high intensity range 10^{14-17}W/cm^2 . It is also seen that few cycle laser pulses are desirable for high absorption in fullerene. Also low Q and moderate intensities has remarkably high absorption. The model can also describe experimental findings on highly intensity sensitive broadband HHG from fullerene molecules¹²⁻¹⁴ owing to its strict few cycle selective response. The model is useful to describe the experimental results in various single layered nanostructures²⁰ interacting with ultrashort laser pulses.

CONCLUSIONS

In summary, non linear absorption of intense few cycle laser pulses ($I < 10^{18} \text{W/cm}^2$) in fullerenes is studied by introducing a rigid shell model. C_{60} is considered as a laser driven nonlinear oscillator. The difference of intense light interaction with C_{60} and solid gas clusters is clearly illustrated. It is proved that the restoring force of fullerene electron shell about the ion shell is constant (for $\Delta < 2R$). This leads to the extraordinary anharmonicity of fullerene at all amplitudes. The electron dephasing with laser at the onset and cluster boundary during oscillations govern the collisionless absorption process. Occurrence of nonlinear resonance in C_{60} is quite different in nature as compared to gas clusters. NLR is easily met at intensities just above the threshold even multiple times during oscillation. Electron cloud does not necessary become free at NLR as compared to NLR in SC. Absorption maximizes in the vicinity above the threshold intensity and critically depends on laser parameters (especially for larger Q and N). For highly ionized fullerene (large Q) absorption is quite high $2-3U_p$ in the high intensity range 10^{14-17}W/cm^2 . The study helps in choosing optimum laser intensity for maximum absorption depending on the ionization in fullerene target.

The formalism can be extended to single layer structures like single walled Carbon Nanotubes and Graphene as well.

ACKNOWLEDGMENTS

The Authors would like to thank Prof. J. A. Chakera, Head Laser Plasma Section (RRCAT) for his useful suggestions and support.

- ¹ G. Kulcsar, D. AlMawlawi, F. W. Budnik, P. R. Herman, M. Moskovits, L. Zhao, and R. S. Marjoribanks, *Physical Review Letters* **84**(22), 5149 (2000).
- ² P. Gibbon and E. Forster, *Plasma Physics and Controlled Fusion* **38**(6), 769 (1996).
- ³ D. F. Price, R. M. More, R. S. Walling, G. Guethlein, R. L. Shepherd, R. E. Stewart, and W. E. White, *Physical Review Letters* **75**, 252 (1995).
- ⁴ U. Chakravarty, V. Arora, P. A. Naik, J. A. Chakera, H. Srivastava, A. K. Srivastava, G. D. Verma, S. R. Kumbhare, and P. D. Gupta, *J. Appl. Phys.* **112**, 053301 (2012).
- ⁵ U. Chakravarty, B. S. Rao, V. Arora, A. Upadhyay, H. Singhal, P. A. Naik, J. A. Chakera, C. Mukherjee, and P. D. Gupta, *Applied Physics Letters* **103**, 054107 (2013).
- ⁶ T. Ditmire, T. Donnelly, A. M. Rubenchik, R. W. Falcone, and M. D. Perry, *Physical Review A* **53**(5), 3379 (1996).
- ⁷ M. Kumar and V. K. Tripathi, *Physics of Plasmas* **20**, 023302 (2013).
- ⁸ M. Kundu and D. Bauer, *Physical Review Letters* **96**, 123401 (2006).
- ⁹ S. V. Fomichev, S. V. Popruzhenko, D. F. Zaretsky, and W. Becker, *Opt. Express* **11**, 2433–2439 (2003).
- ¹⁰ P. Mulser, M. Kanopathipillai, and D. H. H. Hoffmann, *Physical Review Letters* **95**(10), 103401 (2005).
- ¹¹ L. M. Chen, F. Liu, W. M. Wang, M. Kando, J. Y. Mao, L. Zhang, J. L. Ma, Y. T. Li, S. V. Bulanov, T. Tajima, and Y. Kato, *Physical Review Letters* **104**(21), 215004 (2010).
- ¹² R. A. Ganeev, L. E. Bom, J. Abdul-Hadi, M. C. H. Wong, J. P. Brichta, V. R. Bhardwaj, and T. Ozaki, *Physical Review Letters* **102**(1), 013903 (2009).
- ¹³ R. A. Ganeev, C. Hutchison, T. Witting, F. Frank, S. Weber, W. A. Okell, E. Fiordilino, D. Cricchio, F. Persico, A. Zair, J. W. G. Tisch, and J. P. Marangos, *J. Opt. Soc. Am. B* **30**, 7–12 (2013).
- ¹⁴ R. A. Ganeev, H. Singhal, P. A. Naik, J. A. Chakera, A. K. Srivastava, T. S. Dhami, and P. D. Gupta, *Journal of Applied Physics* **106**(10), 103103 (2009).
- ¹⁵ U. Saalman and J. M. Rost, *Physical Review Letters* **91**(22), 223401 (2003).
- ¹⁶ T. Brabec, M. Cote, P. Boulanger, and L. Ramunno, *Physical Review Letters* **95**(7), 073001 (2005).
- ¹⁷ A. Jaron-Becker, A. Becker, and F. H. Faisal, *Physical Review Letters* **96**(14), 143006 (2006).
- ¹⁸ V. R. Bhardwaj, P. B. Corkum, and D. M. Rayner, *Physical Review Letters* **93**(4), 043001 (2004).
- ¹⁹ Q. Lin, J. Zheng, and W. Becker, *Physical Review Letters* **97**(25), 253902 (2006).
- ²⁰ U. Chakravarty, V. Arora, P. A. Naik, J. A. Chakera, H. Srivastava, A. Srivastava, G. D. Varma, S. R. Kumbhare, and P. D. Gupta, *J. Appl. Phys.* **112**, 053301 (2012).